Journal of Theoretical and Applied Mechanics, Sofia, 2014, vol. 44, No. 2, pp. 3–24

GENERAL MECHANICS

IDENTIFICATION OF PEDESTRIAN BRIDGE DYNAMIC RESPONSE TROUGH FIELD MEASUREMENTS AND NUMERICAL MODELLING: CASE STUDIES*

George D. Manolis, Asimina Athanatopoulou-Kyriakou,
Kosmas D. Dragos, Argyris Arabatzis, Alexandros Lavdas
Department of Civil Engineering, Aristotle University,
54124 Thessaloniki, Greece,
e-mails: gdm@civil.auth.gr, minak@civil.auth.gr,
kosmdrag@gmail.com, argarab@gmail.com, alexlavd@hotmail.com

Christos Z. Karakostas
Earthquake Planning and Protection Organization,
55535 Thessaloniki, Greece,
e-mail: christos@itsak.gr

[Received 14 April 2014. Accepted 02 June 2014]

Abstract. In this work, we develop a technique for performing system identification in typical pedestrian bridges, using routine equipment at a minimal configuration, and for cases where actual structural data are either sparse or absent. To this end, two pedestrian bridges were examined, modelled and finally instrumented so as to record their dynamic response under operational conditions. More specifically, the bridges were numerically modelled using the finite element method (FEM) according to what was deduced to be their current operating status, while rational assumptions were made with respect to uncertain structural properties. Next, results from field testing using a portable accelerometer unit were processed to produce response spectra that were used as input to a structural identification software program, which in turn yielded the excited natural frequencies and mode shapes of the bridges. The low level of discrepancy is given between analytical and experimental results, the latter are used for a final calibration of the numerical models.
Key words: Non-destructive testing, pedestrian bridges, modal identification, finite elements, structural dynamics, ambient vibrations.

*Corresponding author e-mail: gdm@civil.auth.gr

1. Introduction

The trend towards lightweight design has had a decisive effect on the pedestrian bridges dynamic behaviour. Reduction of the bridges' mass can be beneficial with respect to their earthquake response, but the subsequent drop in available damping has proven detrimental to their dynamic behaviour under operational conditions. Also, live loads derived from pedestrian traffic are often comparable to the weight of the bridge, especially in case of overcrowding, thus resulting in high amplitude oscillations. Observations on overcrowding conditions have shown that this dynamic overloading can trigger unforeseen modes of vibration, associated with response displacements and accelerations that exceed their respective serviceability criteria and cause discomfort to users. The most indicative example of such an event is the Millennium Bridge in London, whose response to excessive crowding of about 100 000 users during opening day [1], proved disastrous. Pedestrian density reached 1.5 people/m^2 activating lateral and torsion modes that had not been accounted for in the design. Similar case studies were reported for the T-Bridge in Japan due to overcrowding after the end of a sports event [2], and for both the Passerelle-Léopold Sédar-Senghor bridge in Paris and the Alexandra Bridge in Ottawa, Canada due to overcrowding of viewers watching firework festivals [1].

Vibration-based system identification has been employed in numerous studies that address the issue of bridge dynamic behaviour, either using the Force Vibration Testing (FVT) or the Ambient Vibration Testing (AVT) methods. Relevant research in this area has been conducted by Nakamura et al. [3] and by Zivanovic and Pavic [4]. AVT methods have become more prevalent in recent years, primarily because they are easier to set up, especially when it comes to instrumentation of full scale structures. The implementation of output-only data processing techniques, instead of input-output techniques traditionally used in FVT, has been investigated by many researchers, e.g. Cunha et al. [5, 6], De Roeck et al. [7] and Brincker et al. [8, 9]. The use of such test results can be used to enhance the reliability of the numerical models when accurate information regarding structural properties is unavailable or hard to retrieve. Finally, applicability of these methods in updating numerical models, in structural assessment and in structural damage detection has been studied by Cantieni et al. [10].

Design code provisions with regard to pedestrian bridge dynamics are relatively recent and followed major incidents of unanticipated dynamic behaviour, like the amendments to British Standards BS-5400 following the Millennium Bridge incident [1]. In EC1, Part 2 [11], the static load models for design are discussed along with guidelines regarding dynamic effects under operational conditions. Other guidelines for footbridges developed within the framework of major research projects are: SETRA [12], a French Transport Department Agency publication with guidelines on composite steel-concrete bridges for vehicular traffic primarily, and the HIVOSS [13] set of rules on the design of steel footbridges and on measurement techniques regarding their vibrations by a research consortium headed by the University of Aachen in Germany.

In this work, two pedestrian bridges are studied, one serving as a boulevard overpass in the city of Thessaloniki and made of reinforced concrete (R/C), and another being a small suspension bridge over the Pinios river in the Tembi valley of Central Greece with a R/C deck and a steel pylon-cable supporting system. Both footbridges were constructed in the late 1960s-early 1970s, and are still in use today. The former bridge underwent some superficial remedial work in 2009, while the latter one was extensively retrofitted in 2002 by a local contractor. Structural data could only be retrieved for the suspension bridge, whereas only architectural drawings were available for the overpass bridge. The aim of the work presented in this paper is to investigate the possibility of performing system identification using minimal, "‘off-the-shelf"’ monitoring equipment. The measurements from an ambient vibration environment can then be used for updating the background numerical FEM models. This procedure is useful for structures for which information regarding their structural properties is either limited or unavailable. Furthermore, it establishes quite satisfactorily the current "‘state-of-health"’ of the structure, which opens the way for the design and implementation of retrofit strategies.

The present approach has certain limitations. For instance, it cannot account for complex soil behaviour. This would require a separate geotechnical investigation, and this might be necessary if a pedestrian bridge is founded on poor quality soil. However, it can be argued that soil conditions are of minor importance if the bridge deck response is our main concern. The reason is that the bridge deck is influenced by traffic and is usually decoupled to some degree from its supporting piers due to the presence of special connections that are close to simple supports. This is the fact that minimizes soil-structure-interaction effects. Finally, we are examining normal operating conditions, so that the nonlinear soil response is not considered. This fact would be important if extreme loads such as strong earthquakes had to be taken into account.

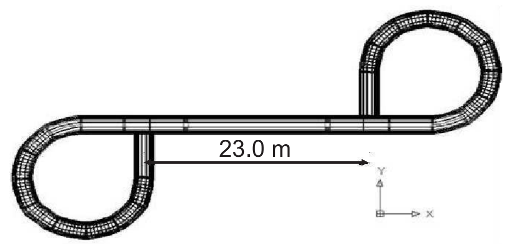

Fig. 1. R/C overpass bridge: (L) General view and (R) top plan view

2. Pedestrian overpass bridge over the Thessaloniki seafront boulevard

As it is shown in Fig. 1, this is a R/C overpass bridge crossing the seafront boulevard in Thessaloniki, Greece. The bridge was built in the early 1970s and comprises three separate segments. The 23.00 m long central span is elevated, rests on two piers and crosses the boulevard. It has two overhanging ends, each attached to a circular spiral ramp that serves for the ascent/descent of pedestrians and bicycles. The deck is a continuous box girder and its continuity is interrupted by two full-depth expansion joints, located in the mid-span of the two bays adjacent to the central span. The piers have variable cross section, starting with a 70×70 cm (height $\times$ width) square section at their base and ending with a rectangular section of 240×70 cm at their top. This section variation is cubic with height, and apart from an aesthetics point of view, enhances lateral stiffness and provides adequate resistance to puncture. The expansion joints are located at the middle of both outer spans adjacent to the central span, and at a distance of 5.80 m from the centroid of each pier, separating the main frame from the spiral ramps. The deck cross-section width remains constant through-out, while the curved slabs serving as ramps rest on piers similar to those of the main frame but with smaller cross section dimensions (70×35; 240×35 cm).

2.1. Finite element modelling and numerical simulations

Modelling assumptions were based on available structural data and on engineering judgment when necessary. The analysis focuses on the central span, which is the most important part of the bridge. The entire model was created using generalised 1D beam finite elements. The influence of each such parameter on the bridge response was investigated as it is given the significant uncertainties regarding both structural and material properties. More specifically, a representative range of values was used for the expansion joint stiffness, for the pier-to-deck connectivity and for the R/C section material degradation. The concrete grade/class was also uncertain and thus, examined parametrically, using values for the modulus of elasticity that correspond to concrete grades in accordance with Greek codes valid during the 1960s. A system of four bored cast-in-place piles was examined as for soil and foundation properties, interconnected with a rigid pile cap, while the range of pile diameters and base levels was also parametrically investigated. The geotechnical profile from a neighbouring site was used, since no site-specific data were available. Other parameters, such as depth of the pile cap, were assigned approximate values according to standard practice at the time of construction. The loads assumed correspond to operational conditions, so that comparison with field

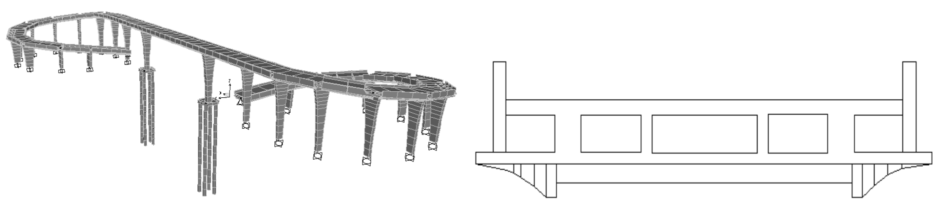

Fig. 2. R/C overpass bridge: (L) FEM model with the foundation piles and (R) deck cross-section details

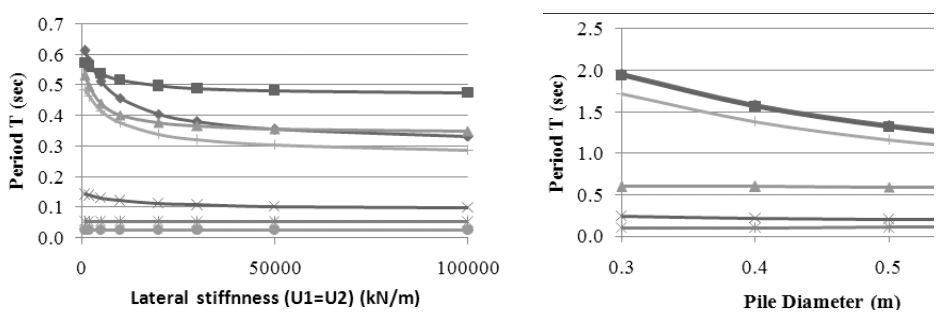

Fig. 3. R/C overpass bridge parametric study investigating the influence of key structural parameters on its fundamental frequencies: (L) Expansion joint stiffness effect and (R) soil flexibility effect manifested in terms of the pile diameters

testing results becomes possible. Numerical modelling of the bridge was carried out using the FEM program SAP 2000 [14] (see Fig. 2). The total bridge mass was derived from both material properties and added loads, while the inertial contribution of the spiral ramps was negligible and no mass was considered.

The influence of each parameter on the natural periods of the structure, and especially those corresponding to the most significant modes of vibration (i.e., those with high participation factors) was thus assessed and some selective results are presented in Fig. 3. An "averaged" model was created judging from the impact of each parameter on the numerical results as the most suitable one for comparison purposes with recordings of the bridge dynamic response under operating conditions. Next, modal analysis results from the "averaged" model are presented in Table 1. These results show that the first two dominant vibration modes are both translational and along the horizontal plane of the deck, i.e., Y-transverse and X-longitudinal and are slightly coupled. The third mode is predominantly torsion, while the fourth mode is translational along the Z (vertical) axis, see Fig. 4. Actual vibration measurements that follow, verify the presence of vertical modes and are used to further calibrate the FEM numerical model.

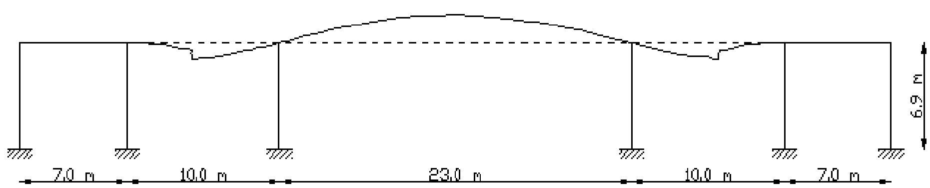

Fig. 4. R/C overpass bridge basic vertical mode of vibration

3. Pedestrian suspension bridge over the Pinios river at Tembi Valley

The Agia Paraskevi footbridge spans the Pinios river flowing through the Tembi valley in central Greece. The bridge was originally built in 1960 and was extensively repaired and retrofitted in 2003. More specifically, it is a 96 m long slender suspension bridge with a central span of 54 m (see Fig. 5). This central span has a cable-suspended composite deck, with longitudinal and transverse steel beams supporting an R/C slab, while the end spans are of prestressed concrete. The bridge deck is 1.65 m wide, but the clear passage width is actually 1.50 m because of the railing.

Table 1. Natural periods (in sec), mass participation ratios (U) and their sums (ΣU) for the first twelve modes of the R/C overpass bridge

Mode No.	Period (sec)	UX	UY	UZ	$\Sigma(UX)$	$\Sigma(UY)$	$\Sigma(UZ)$
1	0.877	0.0275	0.9720	0.0000	0.0275	0.9720	0.0000
2	0.640	0.9723	0.0274	0.0000	0.9998	0.9994	0.0000
3	0.562	0.0000	0.0000	0.0000	0.9998	0.9994	0.0000
4	0.442	0.0000	0.0000	0.3529	0.9998	0.9994	0.3529
5	0.171	0.0002	0.0000	0.0000	1.0000	0.9994	0.3529
6	0.165	0.0000	0.0000	0.5764	1.0000	0.9994	0.9292
7	0.150	0.0000	0.0000	0.0000	1.0000	0.9994	0.9292
8	0.111	0.0000	0.0006	0.0000	1.0000	1.0000	0.9292
9	0.088	0.0000	0.0000	0.0678	1.0000	1.0000	0.9970
10	0.061	0.0000	0.0000	0.0000	1.0000	1.0000	0.9970
11	0.043	0.0000	0.0000	0.0028	1.0000	1.0000	0.9999
12	0.043	0.0000	0.0000	0.0000	1.0000	1.0000	0.9999

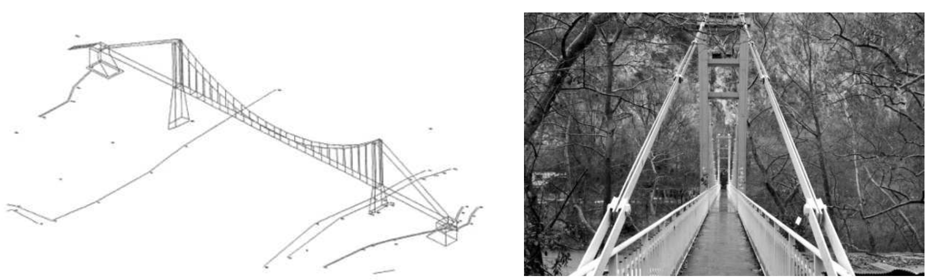

Fig. 5. Tembi valley suspension bridge: (L) General view and (R) Deck details

The end-spans stand today exactly as they were built in 1960 and are continuously connected to the piers. However, the mid-span was demolished and rebuilt in 2003. The mid-span is now connected to the piers by pinned connections and secured in-place through steel and lead blades of total width of 5 cm anchored at the top of the piers. The two main towers are shaped as portals and each is built from two pylons connected by three composite R/C-steel beams at different levels with overall height of 10.2 m. The pylons are composite hollow steel rectangular sections filled with concrete. Each of the two main cables follows a parabolic profile and comprises a series of two parallel steel blades of 2.35 m length, interconnected by pins at their ends.

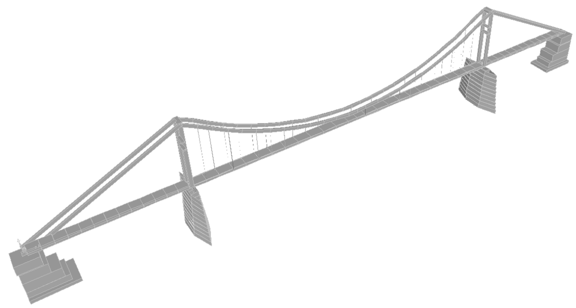

Fig. 6. Tembi valley suspension bridge: 3D FEM model

The cables are anchored to a steel cylindrical seat at the top of each pylon, while their ends are attached to two concrete anchor blocks at the river banks. The vertical hangers consist of reinforcing steel bars 22 mm in diameter. Their top level is suspended from connection points on the main cables with pairs of blades, while their bottom level is fastened to the main beams on the deck. Finally, the footbridge piers are quite massive, so proper load transfer to the ground is assured.

3.1. Finite element modelling and numerical simulations

A 3D model was created using the FEM program SAP 2000 [14], see Fig. 6. The main towers and the pylons were modelled as 1D beam finite elements, while the main cable and the vertical hangers as truss finite elements. Finally, both beam and shell elements were used for modelling the deck. Pre-stressing forces at the two end-span decks were assumed negligible due to structural ageing as far as modelling assumptions are concerned. Geometric non-linearities were accounted for by following Ernst's (1965) principle to use an equivalent modulus of elasticity Eso that the inclined cable's stiffness matrix is equal to that of an equivalent truss element of length L and cross-section area A, taking into consideration the sag effect and the tensile stresses in the cable, see Zivanovic and Pavic [4]. Rigid beam elements were used for modelling of the piers, since their mass, calculated at 880 tn each, is significantly higher than the 110 tn total mass of the deck. Finally, damping was set to 2% following the bridge numerical modelling recommendations, given in Ref. [4]. The model was analyzed as a plane frame in order to produce results compatible with the field measurements and the pier–to-deck connectivity was examined parametrically.

Table 2. The first six modes for the suspension bridge deck under simple support conditions

Mode No.	Period (sec)	Frequency (Hz)	Type of Mode
1	1.5062	0.6639	Mid-span bending and sway
2	0.7021	1.4243	Mid-span bending and sway
3	0.4044	2.4729	Mid-span bending
4	0.3773	2.6503	Mid-span bending and sway
5	0.2539	3.9385	End-span bending and sway
6	0.2538	3.9401	End-span bending

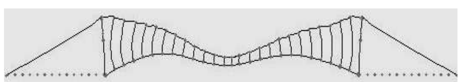

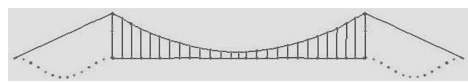

Fig. 7. Tembi valley suspension bridge: (L) Mode shape 3 with mid-span bending, natural period of 0.40 sec and a mass participation ratio of 36%; (R) Mode shape 6 with end-span bending, natural period of 0.25 sec and a mass participation ratio of 25%

Table 3. The first six modes of the suspension bridge for different fixity conditions of the deck to the piers

Mode No.	Period (sec)			Type of Mode
	Complete Fixity	Partial Fixity	Simple Support	
1	0.9552	1.4184	1.5062	Mid-span bending and sway
2	0.5879	0.6874	0.7021	Mid-span bending and sway
3	0.3741	0.4015	0.4044	Mid-span bending
4	0.3063	0.3686	0.3773	Mid-span bending and sway
5	0.2539	0.2539	0.2539	End-span bending and sway
6	0.2538	0.2538	0.2538	End-span bending

In terms of results, Table 2 gives the first six modal shapes of the suspension bridge, for a simple (pin) support of the mid-span to the piers. Next, Fig. 7 plots the two modal shapes with the largest mass participation ratios in the vertical Z-axis. Finally, Table 3 gives results for the first six natural periods of the bridge and the corresponding type of mode. These are presented for alternative numerical models created to simulate the connection between the central deck and its supporting piers, using link elements in lieu of either complete or zero fixity. The link element characteristics were decided upon through a trial and error process. It is obvious in Table 3, that the modelling assumptions regarding the connections mentioned above did not alter the basic type of modal shapes, though they did change the natural period values.

4. Experimental assessment of modal data under operational conditions

Evaluation of the actual dynamic characteristics of civil engineering structures under service conditions through measurements of their dynamic response has been attracting research effort worldwide, see Crocker [15]. Measured response data for bridges from both ambient and forced vibrations offer an opportunity to examine, both quantitatively and qualitatively, their dynamic behaviour for low and medium level vibrations, see De Roeck et al. [7] and Ntotsios et al. [16]). As mentioned, there has been a growing trend in recent years towards ambient vibration testing in the field of experimental modal analysis [17–22]. There are several reasons for this, for instance, testing is fast and inexpensive, since extra equipment for producing forced excitations is unnecessary. Also, these methods are easily applicable to structures that would otherwise demand high energy input to exhibit measurable oscillations. Finally, testing is often conducted without disrupting the operation of the structure, an important point for bridges. The added advantage is that the recorded response is representative of real operational conditions. The basic concept behind ambient vibration testing is that excitations induced by random external actions under operational conditions can be idealized as Gaussian 'white noise', with uniform frequency content across the bandwidth of interest. Output-only methods are employed for modal identification since input energy is unknown, i.e., computation of natural frequencies, modal shapes and damping ratios from the recorded response.

Estimation of the modal characteristics using ambient vibration data is based on a least-squares minimization of the measure of fit as:

$$E(\psi) = \sum_{k=1}^{N_\omega} tr\left[\left(S(k\Delta\omega;\psi) - \widehat{S}(k\Delta\omega)\right)^{*T}\left(S(k\Delta\omega;\psi) - \widehat{S}(k\Delta\omega)\right)\right], \tag{1}$$

between the cross-power spectral density (CPSD) matrix $\widehat{S}(k\Delta\omega) \in C^{N_0\times N_0}$, estimated from the measured output acceleration time histories and the CPSD matrix $S(k\Delta\omega;\psi) \in C^{N_0 \times N_0}$, predicted by modal analysis. In the above, N_0 is the number of measured DOF, $\Delta\omega$ is the discretization step in the frequency domain, $k = \{1, \cdots, N_\omega\}$ is the index set corresponding to discrete frequency values $\omega = k\Delta\omega$, N_ω is the number of data in the indexed set, and ψ is the parameter set to be estimated.

The equipment used for the field measurements in this work comprised two uniaxial accelerometers, an interface unit for signal conditioning, a power supply unit, a portable computer for data storage and processing, plus ancillary equipment in the form of cables, connectors, triggers, etc. This equipment is rather inexpensive and is also used for demonstrations in our graduate-level program on earthquake-resistant design of structures.

More specifically, the interface unit can support up to four recording channels. Next, the transducers are connected to the sensor interface (which handles the AC to DC (alternating current to direct current) current conversion) and the digitized raw data are then transferred through a USB cable equipped with noise reduction filters to the computer, which is used as a recording unit. The uniaxial acceleration transducers are of type KYOWA ASW-A, see Ref. [23], with waterproof stainless steel coating that provides corrosion protection. The compatible sensor interface is of type KYOWA PCD-300A [23], offering 12-bit A/D conversion, a full-scale strain measurement range of $10000{\cdot}10^{-6}$ and a maximum sampling frequency of 5 kHz. During measurements, one of the accelerometers is used as 'reference sensor' and is kept in place for the entire recording procedure, while the other 'roving sensor' is moved around to measure the response at various locations along the bridge longitudinal axis.

4.1. Data processing for modal identification

Two different techniques are used for evaluation of the excited modes of the instrumented bridges, namely the Curve-fit Frequency Domain Decomposition (CFDD) and the Stochastic Subspace Identification–Canonical Variant Analysis (SSI-CVA), see Brincker et al. [8]. The CFDD technique is an extension of the Frequency Domain Decomposition (FDD) technique, where the key idea is to perform an approximate decomposition of the system response into a set of independent single degree-of-freedom (SDOF) systems, one for each mode. This process is performed by decomposing each of the estimated spectral density matrices into constituent SDOF parts. It can be shown, that the singular values are estimates of the auto spectral density of the SDOF systems, and the singular vectors are estimates of the mode shapes. In the CFDD, an extra step is taken that leads to estimation of both the frequency and damping ratios from the SDOF spectral bells using a frequency domain, curve fitting technique. It is noted, that FDD methods require an interactive peak-picking stage from the user. On the other hand, the SSI techniques use a parametric model, which is directly 'fitted' to the time-series data, as recorded by the sensors. In particular, the SSI-CVA technique is more effective at estimating modes with a large difference in their energy level (i.e., lowly excited modes interspersed with highly excited ones). A more detailed analysis on the theoretical background behind these techniques can be found in Ref. [8].

5. Thessaloniki overpass R/C bridge instrumentation and data collection

The footbridge crossing the seafront boulevard in Thessaloniki was instrumented for evaluation of its dynamic behaviour under operational conditions using the equipment described above. Measurements are focused primarily on the vertical excitation of the deck due to pedestrian traffic. The location of the reference sensor was selected based on the results of the FEM simulations by SAP 2000 [14], so as not to coincide with a modal node for the dominant modes of vibration. This sensor was eventually placed at 3L/8 from the right pier centroid (L being the deck's pier-to-pier length), where modal amplitude is non-zero for all modes of interest. The rest of the measuring stations (i.e., sensor locations) were at $L/8$ intervals, as shown in Fig. 8, with station 6 being the location of the reference sensor at a distance of 8.625 m from the right pier centroid (designated as station 3). It should be noted, that the instrumentation layout is not symmetrically spread across the span of the bridge (with stations 1 and 2 on one of the overhanging ends of the deck, see Fig. 8),

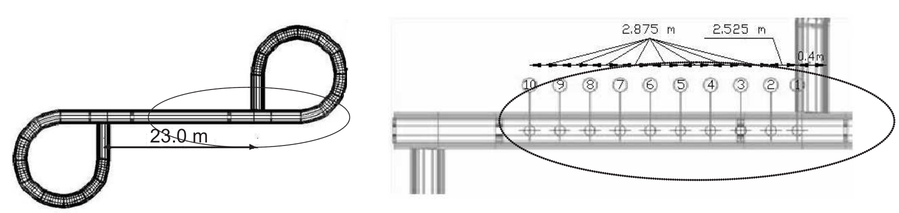

Fig. 8. R/C overpass bridge: (L) Data collection stations and (R) their numbering along the central span

Fig. 9. R/C overpass bridge: (L) Sensor placement for vertical motions and (R) measurement station at $L/8$ and reference sensor at $3L/8$, where L is the deck length

but is nevertheless sufficient for the evaluation of either the symmetric or the anti-symmetric mode shapes of the deck. Vertical vibration response records of approximately 15 min duration were then collected. These data sets for the deck response were eventually divided in two parts, a 6 min time window due to random pedestrian traffic excitation (see Fig. 9) at various frequencies and amplitudes (a few people walking at different pace or running) and a 9 min window of vibration induced solely by vehicular traffic on the boulevard below.

Response records showed that because of recording equipment resolution, significant response was measured only for the case of pedestrian traffic excitations, especially running. This type of measurement falls into the ambient vibration testing category, so the previously mentioned data processing techniques are employed, including both time and frequency domain analysis methods. A quick, first stage processing of the results was conducted at the beginning of the testing session which lasted three days, so as to gain insight on the bridge response. Finally, a more elaborate, second stage computer analysis followed, which led to the final modal identification results.

5.1. Overpass bridge preliminary response analysis

First stage data processing was performed using the SeismoSignal [24] software. This involved baseline correction of the raw time series and filtering with a Butterworth band-pass filter applied between 0.1–20 Hz. Next, the Fourier spectra and the Power Spectral Density (PSD) functions of the corrected time history response records were obtained. Figure 10 plots typical processed data from Station 8 located at a distance of 5L/8 along the deck

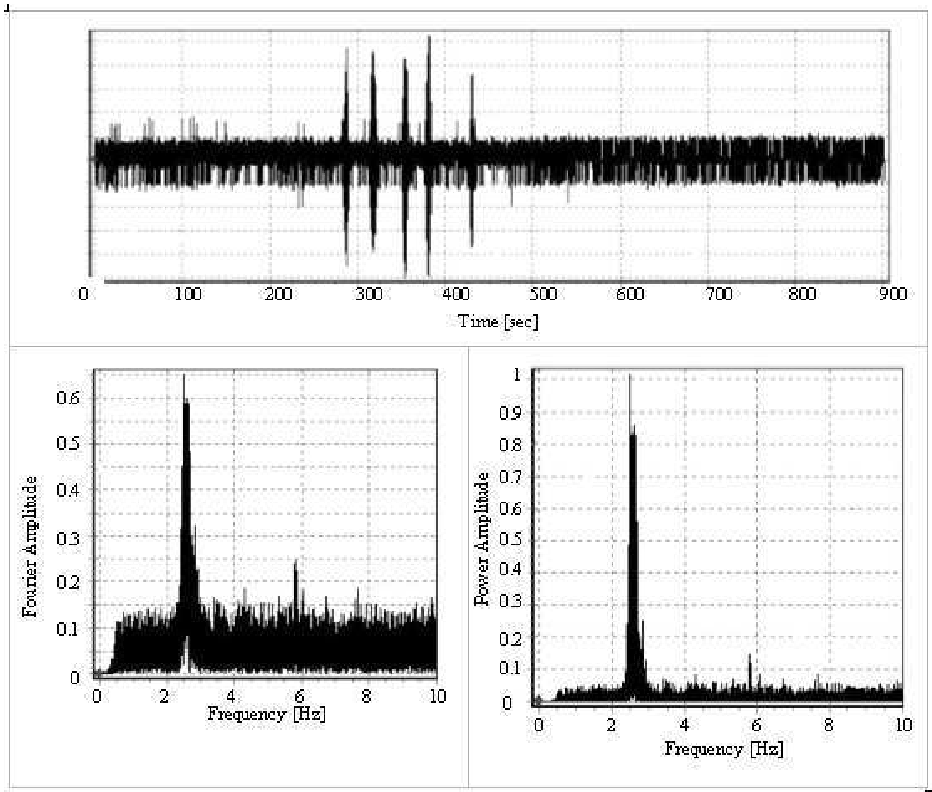

Fig. 10. R/C overpass bridge: (T) Corrected time series for station at station $5L/8$, (L) Fourier spectrum at station $5L/8$ and (R) PSDF for the reference station at $3L/8$

length. A brief look at the spectrum shape, focusing on possible amplitude and phase angle shifts between the reference point and the measuring station, gives a first insight on the dynamic behaviour of the structure by identifying spectral peaks as potential eigen frequencies. More specifically, the top graph in Fig. 10 illustrates the corrected total (15 min) time history response, where it is obvious that the highest acceleration values occur within a specified time window that corresponds to intense pedestrian traffic (i.e., running) and produces peak amplitudes in the Fourier spectrum and in the PSD function. More specifically, the Fourier spectrum peaks at a frequency of approximately 2.65 Hz. Along with similar amplitude and phase shifts between the reference point and its symmetric point at Station 8, these peaks are indicative of the fundamental vertical mode of vibration, which is characterized by a sinusoidal shape that is symmetric about the deck center. Further data processing, however, is impossible without the aid of specialized software.

5.2. Overpass bridge modal identification

The recorded vertical response of the bridge at the pre-selected sensor locations was used to identify its modal characteristics through processing with the ARTeMIS Extractor software package [25]. Figure 11 is the geometric model of the bridge, with nodes corresponding to the actual sensor locations (see Fig. 8) and arrows indicating the positive vertical direction of the recorded response. As already mentioned, the instrumentation layout is not symmetrically placed across the span of the bridge, but is nevertheless sufficient for evaluation of either the symmetric or the anti-symmetric mode shapes of the deck. Some intermediate results are shown in Fig. 12 from the FDD method, which requires

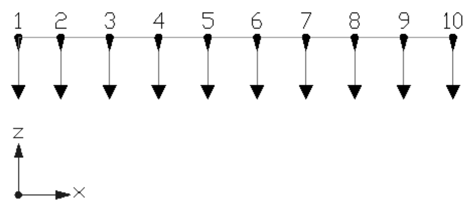

Fig. 11. R/C overpass bridge: Geometric model numbering for the ARTeMIS extractor software

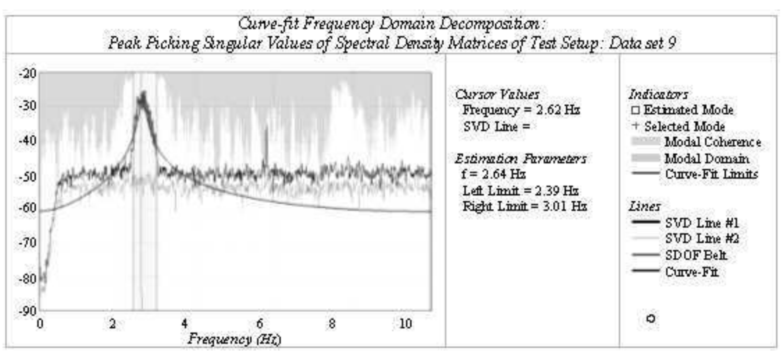

Fig. 12. Evaluation of a particular mode using the Peak Picking–FDD method for the R/C overpass bridge

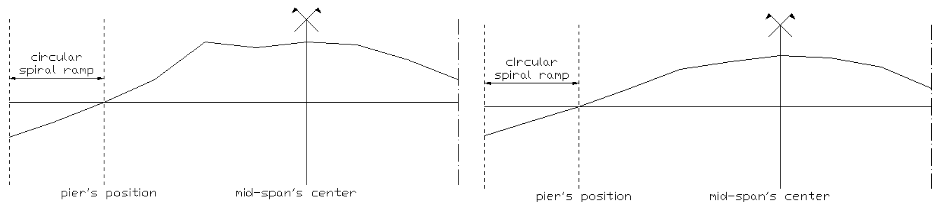

Fig. 13. R/C overpass bridge first eigenvector computation by (L) the Curve-fit FDD and (R) the SSI-CVA methods

an interactive peak-picking stage from the user. It was possible to estimate the first vertical mode of the deck using the instrumentation procedure described herein, see Fig. 13. As seen in these plots, the mode shapes are similar, and even better agreement is recovered for the estimated natural frequency (2.616 Hz from CFDD versus 2.626 Hz from SSI-CVA). These values are also in good agreement with the results of the FEM numerical model described previously.

5.3. Overpass bridge comparison of experimental and analytical results

The next stage involves a comparison between numerical and experimental results. More specifically, the first estimated vertical mode of the 'averaged' FEM model possesses a natural period of $T = 0.442$ sec, while the period of the corresponding experimentally evaluated mode is $T = 1/2.626 = 0.385$ sec. The difference between these values is about 10% and their mode shapes are similar, both being sinusoidal and symmetric about the center of the deck. As already mentioned, vibrations induced by vehicular traffic under the bridge did not produce measurable oscillations. This can be attributed to the large mass and damping of the bridge piers, which demands high energy input in order to sufficiently excite the deck through motion of the piers. Higher modes of vibration along the vertical axis, as well as all modes along the horizontal plane, could not be identified. This is mainly due to low energy input by both pedestrians and vehicles, in combination with the rather low resolution capabilities of the recording system.

6. Pinios River suspension bridge instrumentation and data collection

A parallel experimental investigation was conducted for the Agia Paraskevi footbridge (see Fig. 14) spanning the river Pinios at Tembi valley by

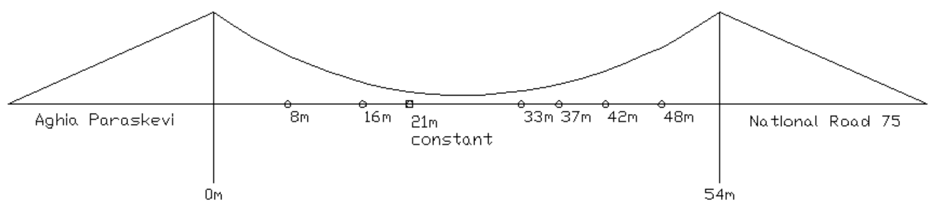

Fig. 14. Tembi valley suspension bridge: Location of recording stations along the span

using the same testing equipment. As before, the objective was to evaluate the footbridge modal properties through its response to pedestrian-induced loading. Measurements were made for vertical (Z-axis) accelerations at mid-span only. The recording procedure, plus the selection of the reference and moving sensor locations (stations) along the deck, followed the same reasoning used for the instrumentation of the Thessaloniki overpass R/C bridge. More specifically, one of the two available transducers was set at a fixed recording location (the reference station), while the second one was sequentially placed at pre-selected locations along the bridge span for each recording session. All recording sessions were of 10–15 min duration. Figure 14 also depicts the six locations of the recording stations along the bridge span, all selected so as to avoid a 'node' (i.e., a zero-crossing point) in the first few fundamental modes. Thus, stations at 1/2, 1/3, 2/3, 1/4 and 3/4 of the length of the mid-span were rejected. The reference transducer (at 21 m from the left pier, see Fig. 14) was placed as far as possible from likely nodes of these first modes, in order for modal amplitudes to be as large as possible. The recordings were from the random (asynchronous) pedestrian traffic, as tourists were crossing the bridge during late spring and under excellent weather conditions.

6.1. Suspension bridge data processing

The recordings were made over two working days and were used to estimate the excited modes of the bridge. The ARTeMIS Extractor [25] software package was employed, along with the FDD technique described previously. From the data collected, it was possible to estimate the excited vertical modes of the deck, which are listed in Table 4. Next, Fig. 15 plots the corresponding peak-picking stage of the FDD technique. It is observed that significant experience is required from the user in order to identify peaks that correspond to actual structural modes, which are based on various criteria whose description

Table 4. Field measurements versus FEM simulations for the suspension bridge

Field measurements	***Numerical simulation***
Period: 0.768 sec 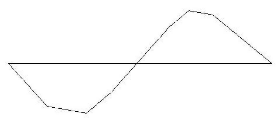	***1st Mode*** Period (continuous span): 0.955 sec Period (simply supported span): 1.506 sec 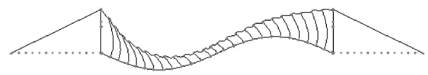
Period: 0.454 sec 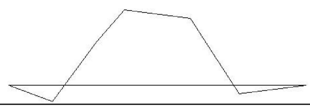	***2nd Mode*** Period (continuous span): 0.588 sec Period (simply supported span): 0.702 sec 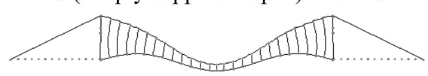
Period: 0.312 sec 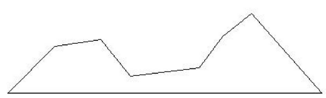	***3rd Mode*** Period (continuous span): 0.374 sec Period (simply supported span): 0.404 sec 
Period: 0.236 sec 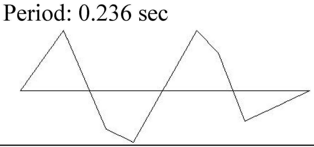	***4th Mode*** Period (continuous span): 0.297 sec Period (simply supported span): 0.311 sec 
Period: 0.067 sec 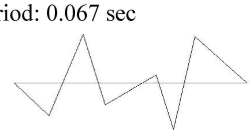	***5th Mode*** Period (continuous span): 0.169 sec Period (simply supported span): 0.144 sec 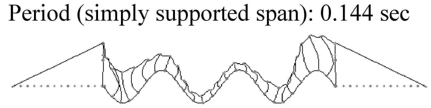

falls beyond the scope of the present work.

6.2. Suspension bridge comparison with FEM simulations

After evaluating the experimental results and comparing with the corresponding numerical model investigations (see Table 4), the following points can now be deduced: (a) The shape of the first five modes from the field measurements coincide with the corresponding shapes from the numerical FEM simulations; (b) The FEM model turned out to be more flexible than the actual bridge, since the natural periods of all analytical mode shapes are greater

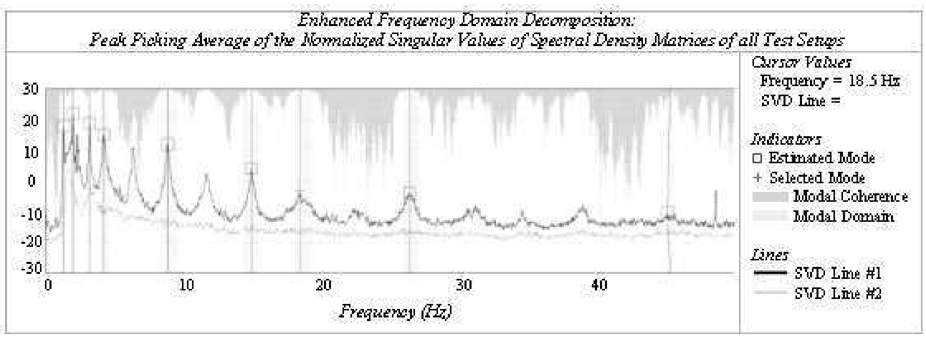

Fig. 15. Tembi valley suspension bridge: Fourier spectrum for span vibrations

than the corresponding periods identified from the field measurements; (c) The first mode shape of the mid-span is the familiar sinusoidal mode shape of a simply supported beam. Moreover, it is the mode shape with the largest mass participation ratio, numerically estimated at about 35%. (d) The third mode shape of the central deck has no zero-crossing point; (e) The natural period values for the central deck recovered from the FEM model are greatly influenced by the assumed type of connection between deck and piers. Following rather extensive parametric investigations, it turned out that the results of the numerical modelling are closer to the field measurement if we assume a rigid connection of the deck to the pier.

7. Summary and Conclusions

Two pedestrian bridges are examined in this work in terms of their dynamic behaviour. The first is a R/C overpass spanning a major urban boulevard, while the second is a composite suspension bridge spanning a river valley. The possibility of performing system identification using minimal equipment and in the absence of reliable structural data (as in the case of the first bridge) was investigated. Numerical analysis using the FEM was followed by field testing under operational conditions and modal extraction after suitable data processing. A general conclusion is that despite the limitations of the available recording equipment, the uncertainties in the numerical modelling plus the difficulties associated with data collection, the dynamic properties of the two footbridges were reliably identified based on comparisons between numerical and experimental results.

More specifically, normal operating conditions are assumed, which implies a 'serviceability limit state' for the pedestrian bridges. The important factors here are concrete creep and shrinkage for R/C bridges, metal fatigue for steel bridges and foundation settlement of the piers. It is only under extreme loads such as earthquakes that non-linear soil and structural behaviour becomes important, but this lies outside the present considerations. Observations on the response of the Via Egnatia highway bridge network built over the last two decades in Northern Greece [16], point out that the exact soil profile and foundation details for these bridges does not influence the deck dynamic response under normal operating conditions induced by vehicular traffic.

In closing, the present methodology can be implemented for monitoring and assessing the normal operating condition of several types of bridges, which is useful information for an initial planning of retrofit strategies. This is achieved by first, performing an evaluation of their current operating conditions, and then utilizing the experimentally obtained data for calibration of the numerical model that was set up based on structural data deduced from the initial design.

REFERENCES

[1] Dallardal, P., T. Fitzpatrick, A. Flint, A. Low, R. Ridsdill-Smith, M. Willford, M. Roche. London Millennium Bridge: Pedestrian-induced Lateral Vibration. *ASCE J. Bridge Eng.,* **6** (2001), No. 6, 412–417.

[2] Fujino, Y., B. M. Pacheco, S. I. Nakamura, P. Warnitchal. Synchronization of Human Walking Observer during Lateral Vibration of a Congested Pedestrian Bridge. *Earthquake Eng. Struct. Dyn.,* **22** (1993), No. 9, 741–758.

[3] Nakamura, S. I. Model for Lateral Excitation of Footbridges by Synchronous Walking. *ASCE J. Struct. Eng.,* **130** (2004), No. 1, 32–37.

[4] Zivanovic, M., A. Pavic. Dynamic Response due to Vertical Load Models of Pedestrians, *In: Proceedings of the 8th EURODYN International Conference on Structural Dynamics*, 4–6 July 2011, Belgium, Leuven.

[5] Cunha, A., E. Caetano. Experimental Modal Analysis of Civil Engineering Structures. *Sound and Vibration*, **6** (2006), No. 40, 12–20.

[6] Cunha, A., E. Caetano, R. Brincker, P. Andersen. Identification from the Natural Response of the Vasco da Gama Bridge, In: Proceedings of the 22nd International Modal Analysis Conference IMAC, USA, Dearborn, Michigan, 2004, 202–209.

[7] De Roeck, G., B. Peeters, J. Maerck. Dynamic Monitoring of Civil Engineering Structures, In: Proceedings of Computational Methods for Shell and Spatial Structures, IASS-IACM 2000 Conference, Greece, Athens, 2000, 1–24.

[8] Brincker, R., L. Zhang, P. Andersen. Modal Identification from Ambient Responses using Frequency Domain Decomposition, In: Proceedings of the 18th International Modal Analysis Conference IMAC, Society of Experimental Mechanics, USA, Texas, San Antonio, 2000, 625–630.

[9] Brincker, R., L. Zhang. Frequency Domain Decomposition Revisited, In: Third International Operational Modal Analysis Conference, 2009, Italy, Ancona, 615–626.

[10] Cantieni, R., M. Brehm, V. Zabel, T. Rauert, B. Hoffmeister. Ambient Testing and Model updating of a Bridge for High-speed Trains, In: Proceedings of the 25th International Modal Analysis Conference IMAC, February 4–7 2008, USA, Florida, Orlando, 1005–1013.

[11] CEN EC1-2. Actions on Structures. Part 2: Traffic Loads on Road Bridges and Footbridges, European Committee for Standardization, 2003, Brussels, Belgium.

[12] Setra. Service d' Etudes sur les Transports, Steel Concrete Composite Bridges: Sustainable Design Guide, 2010, France, Bagneux, SETRA, (downloaded electronically).

[13] Hivoss. Human Induced Vibrations of Steel Structures, Design of Footbridges, I: Background, II: Guidelines. Report No. RFS2-CT-2007-00033, 2007, Germany, Aachen, Aachen University, (downloaded electronically).

[14] Sap. (Structural Analysis Program). Integrated Finite Element Analysis and Design of Structures, 2000, CSI Inc., USA, California, Berkeley, (downloaded electronically).

[15] Crocker, M. J. Handbook of Noise and Vibration Control, USA, Hoboken, New Jersey, John Wiley, 2007.

[16] Ntotsios, E., C. Karakostas, V. Lekidis, P. Panetsos, I. Nikolaou, C. Papadimitriou, T. Salonikios. Structural Identification of Egnatia Odos Bridges based on Ambient and Earthquake Induced Vibrations. *Bull. Earthquake Eng.*, **7** (2009), No. 2, 485–501.

[17] Peeters, B., G. De Roeck. Reference-based Stochastic Subspace Identification for Output-only Modal Analysis. *Mech. Systems and Signal Processing*, **13** (1999), No. 6, 855–878.

[18] Peeters, B., G. De Roeck. Stochastic System Identification for Operational Modal Analysis: A review. *J. Dyn. Systems ASME,* **123** (2001), No. 4, 659–667.

[19] Basseville, M., A. Benveniste, M. Goursat, L. Hermans, L. Mevel, H. Van Der Auweraer. Output-only Subspace-based Structural Identification: From Theory to Industrial Testing Practice. *J. Dyn. Syst. ASME*, **123** (2001), No. 4, 668–676.

[20] Verboven, P. Frequency Domain System Identification for Modal Analysis, PhD Thesis, Belgium, Brussels, Vrije Universiteit, 2002.

[21] Gauberghe, B. Applied Frequency-domain System Identification in the Field of Experimental and Operational Modal Analysis, PhD Thesis, Belgium, Brussels, Vrije Universiteit, 2004.

[22] Peeters, B., H. Van Der Auweraer. Recent Developments in Operational Modal Analysis, In: Proceedings EURODYN 2005, edited by C. Soize and G. I. Schueller, Netherlands, Rotterdam, Millpress, 2005, 149–154.

[23] Kyowa Sensor Interface PCD-300A. Hardware Instruction Manual, KYOWA Electronic Instruments Co. Ltd., Japan, Tokyo, 2009.

[24] Seismosignal, Version 4.0. Earthquake Engineering Software Solutions, SeismoSoft Ltd., Italy, Pavia, 2010.

[25] ARTeMIS Extractor. Structural Vibration Solutions, Electronic User's Manual, Denmark, Aarhus, Aarhus University, 2006.